

New Method to Measure Packing Densities of Self-Assembled Thiolipid Monolayers

Julia Kunze,[†] Jay Leitch,[†] Adrian L. Schwan,[†] Robert J. Faragher,[†] Renate Naumann,[‡] Stefan Schiller,[‡] Wolfgang Knoll,[‡] John R. Dutcher,[§] and Jacek Lipkowski^{*,†}

Department of Chemistry, University of Guelph, Guelph, Ontario, N1G2W1 Canada, Max Planck Institut für Polymerforschung, Mainz, Germany, and Department of Physics, University of Guelph, Guelph, Ontario, N1G2W1 Canada

Received December 31, 2005. In Final Form: April 2, 2006

For a monolayer of 2,3-di-phytyl-sn-glycerol-1-tetraethylene glycol-D,L-a-lipoic acid ester lipid (DPTL) self-assembled (SAM) at a gold electrode surface we propose a new method to determine the charge number per adsorbed molecule and the packing density (area per molecule) in the monolayer. The method relies on chronocoulometry to measure the charge density at the SAM covered gold electrode surface. Two series of measurements have to be performed. In the first series, charge densities are measured for a monolayer transferred from the air–solution to the metal–solution interface using the Langmuir–Blodgett (LB) technique. This series of measurements allows one to determine charge numbers per adsorbed DPTL molecule. The second series is performed using a gold electrode covered with a self-assembled monolayer. The charge densities obtained in this series are then used to calculate the packing density with the help of charge numbers per adsorbed DPTL determined in the first series. The area per adsorbed molecule determined by the new method was compared to the area per molecule determined by the popular reductive desorption method. The molecular area determined with the new method is about 20% larger than the area calculated from the van der Waals model, which is a physically reasonable result. In contrast, the popular reductive desorption method gives an area per molecule 20% lower than the minimum estimated based on a van der Waals model. This is a physically unreasonable result. It is also shown that the charge numbers per adsorbed molecule depend on the electrode potential and may assume values smaller than the number of electrons participating in the reductive desorption step. An explanation of the origin of the “partial charge numbers” is provided. We recommend the new method be used in future studies of thiol adsorption at metal surfaces.

1. Introduction

Tethered lipid bilayers have been a subject of a number of recent studies.^{1–12} They are built from thiolipids^{13–20} consisting of a lipid tail and a hydrophilic spacer and are attached to the

solid substrate via a mercapto-linker functionality. Self-assembled monolayers of such molecules are supposed to form an amphiphilic film with a hydrophilic sub-membrane space, mimicking the cytosol of a mammalian cell. The bilayer is then formed by spreading a monolayer of phospholipids onto the monolayer of the thiolipid. Bilayers with such properties can be employed in basic research of transmembrane proteins^{6,7,21–24} and also for development of biosensors.^{1,2}

The present work describes the study of an archaea analogue amphiphilic thiolipid 2,3-di-phytyl-sn-glycerol-1-tetraethylene glycol-D,L-a-lipoic acid ester lipid (DPTL) shown in Figure 1. The molecule has a lipoic acid headgroup containing a cyclic disulfide functionality. This headgroup acts as tether and each sulfur chemically adsorbs on the Au surface. The middle part of the DPTL molecule consists of a tetra-ethylene glycol spacer with four ethylene glycol units. The function of the ethylene glycol part of the molecule is to form the hydrated sub-phase serving as a water reservoir in the model membrane system. The tail of the molecule consists of two isoprenoid chains that each carry four isoprene units. These phytanyl chains are highly hydrophobic and are characterized by a very high chemical stability.

* Corresponding author: E-mail: lipkowski@chembio.uoguelph.ca. Fax: 001-519-7464806.

[‡] Max Planck Institut für Polymerforschung.

[§] Department of Physics, University of Guelph.

[†] Department of Chemistry, University of Guelph.

(1) Sinner, E. K.; Knoll, W. *Curr. Opin. Chem. Biol.* **2001**, *5*, 705.

(2) Knoll, W.; Frank, C. W.; Heibel, C.; Naumann, R.; Offenhäuser, A.; Rühle, J.; Schmidt, E. K.; Shen, W. W.; Sinner, A. *Rev. Mol. Biotechnol.* **2000**, *74*, 137.

(3) Becucci, L.; Moncelli, M. R.; Naumann, R.; Guidelli, R. *J. Am. Chem. Soc.* **2005**, *127*, 13316.

(4) Lang, H.; Duschl, C.; Vogel, H. *Langmuir* **1994**, *10*, 197.

(5) Cornell, B. A.; Braach-Maksvytis, V. L. B.; King, L. G.; Osman, P. D.; Raguse, J.; Wiczorek, L.; Pace, R. J. *Nature* **1997**, *387*, 580.

(6) Naumann, R.; Schmidt, E. K.; Jonczyk, A.; Fendler, K.; Kadenbach, B.; Liebermann, T.; Offenhäuser, A.; Knoll, W. *Biosens. Bioelectron.* **1999**, *14*, 651.

(7) Naumann, R.; Baumgart, T.; Gräber, P.; Jonczyk, A.; Offenhäuser, A.; Knoll, W. *Biosens. Bioelectron.* **2002**, *17*, 25.

(8) Sackmann, E. *Science* **1996**, *271*, 43.

(9) Stelze, M.; Weissmüller, G.; Sackmann, E. *J. Phys. Chem.* **1993**, *97*, 2974.

(10) McConnel, H. M.; Watts, T. H.; Weis, R. M.; Brian, A. A. *Biochim. Biophys. Acta* **1986**, *864*, 94.

(11) Guidelli, R.; Aloisi, G.; Becucci, L.; Dolfi, A.; Moncelli, M. R.; Buoninsegni, F. T. *J. Electroanal. Chem.* **2001**, *504*, 1.

(12) (a) Naumann, R.; Walz, D.; Schiller, S. M.; Knoll, W. *J. Electroanal. Chem.* **2003**, *550–551*, 241. (b) Becucci, L.; Moncelli, M. R.; Naumann, R.; Guidelli, R. *J. Am. Chem. Soc.* **2005**, *127*, 13316.

(13) Woodhouse, G. E.; King, L. G.; Wiczorek, L.; Cornell, B. A. *Faraday Discuss.* **1998**, *111*, 247.

(14) Vanderah, D. J.; Meuse, C. W.; Silin, V.; Plant, A. L. *Langmuir* **1998**, *14*, 6916.

(15) Vanderah, D. J.; Pham, C. P.; Springer, S. K.; Silin, V.; Meuse, C. W. *Langmuir* **2000**, *16*, 6527.

(16) Lang, H.; Duschl, C.; Vogel, H. *Langmuir* **1994**, *10*, 197.

(17) Kryszinski, P.; Zebrowska, A.; Michota, A.; Bukowska, J.; Becucci, L.; Moncelli, M. R. *Langmuir* **2001**, *17*, 3852.

(18) Williams, L. M.; Evans, S. D.; Flynn, T. M.; Marsh, A.; Knowles, P. F.; Bushby, R. J.; Boden, N. *Langmuir* **1997**, *13*, 751.

(19) Cornell, B. A.; Krishna, G.; Osman, P. D.; Pace, R. J.; Wiczorek, L. *Biochem. Soc. Trans.* **2001**, *29*, 613.

(20) Krishna, G.; Schulte, J.; Cornell, B. A.; Pace, R.; Wiczorek, L.; Osman, P. D. *Langmuir* **2001**, *17*, 4858.

(21) Becucci, L.; Guidelli, R.; Liu, Q.; Bushby, R. J.; Evans, S. D. *J. Phys. Chem. B* **2002**, *106*, 10410.

(22) Krueger, S.; Meuse, C. W.; Majkrzak, C. F.; Dura, J. A.; Berk, N. F.; Tarek, M.; Plant, A. L. *Langmuir* **2001**, *17*, 511.

(23) Glazier, S. A.; Vanderah, D. J.; Plant, A. L.; Bayley, H.; Valincius, G.; Kasianovic, J. J. *Langmuir* **2000**, *16*, 10428.

(24) Madhusudhana, N.; Silin, V.; Ridge, K. D.; Woodward, J. T.; Plant, A. L. *Anal. Biochem.* **2002**, *307*, 117.

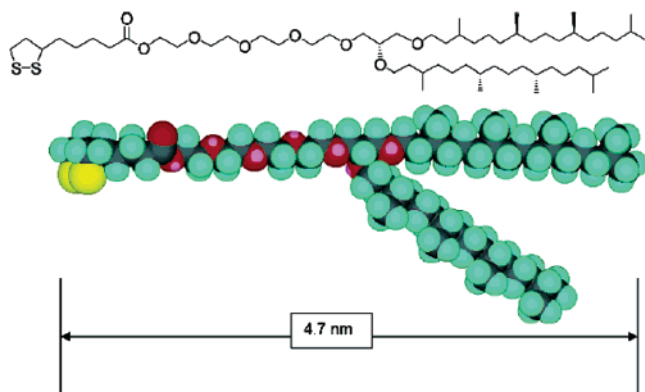
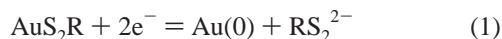


Figure 1. (a) General model of the DPTL molecule showing its three main sections.

Various techniques have already been applied to study monolayers and bilayers of DPTL formed by spreading phospholipid vesicles onto a monolayer of DPTL. The thickness of these layers has been measured using surface plasmon resonance spectroscopy (SPR) and quartz crystal microbalance measurements, the electrical properties have been studied with electrochemical impedance spectroscopy (EIS),¹² and preliminary reflection absorption FTIR measurements of the DPTL films at a gold substrate have been performed in air.²⁵

The objective of the present work was to develop a new method to measure coverage and charge number per adsorbed thiolipid molecule in a monolayer of DPTL self-assembled on a gold electrode surface. Previously, the so-called reductive desorption method has been used to determine the area per DPTL molecule at a gold electrode surface. However, the contribution due to the charging current has not been taken into account, due to uncertainties in the *pzc*s of both the template stripped gold (TSG) and the TSG covered with SAM and uncertainties due to the differential capacitance of the TSG used in this study.²⁵

In the reductive desorption method, one applies a linear voltage sweep from a potential at which the gold electrode is covered by a monolayer of the thiolipid to a sufficiently negative potential at which the thiolipid is desorbed from the gold surface and a voltammetric curve is recorded. Next the voltammetric curve is integrated to give the charge corresponding to the desorption of the thiolipid $\Delta\sigma$. It is assumed that the desorption has a reductive character and that two electrons must be supplied to desorb the dithiol molecule according to the reaction



The coverage Γ is then calculated assuming that $\Delta\sigma = 2F\Gamma$, where F is the Faraday constant. This method is described in detail in refs 26–28.

For a DPTL monolayer assembled at a gold electrode surface, the area per molecule determined by this method corresponds to 58 Å² which is smaller than the area estimated with the help of a space filling model. This result is physically unrealistic and shows that systematic errors due to the uncertainties²⁸ of the charging current correction are involved in the reductive desorption method.

(25) Naumann, R.; Schiller, S.M.; Giess, F.; Grohe, B.; Hartman, K.B.; Karcher, I.; Koper, I.; Lubben, J.; Vasilev, K.; Knoll, W. *Langmuir* **2003**, *19*, 5435.

(26) Widrig, C. A.; Chung, C.; Porter, M. D. *J. Electroanal. Chem.* **1991**, *310*, 335.

(27) (a) Yang, D. F.; Wilde, C. P.; Morin, M. *Langmuir* **1996**, *12*, 6570. (b) Yang, D. F.; Wilde, C. P.; Morin, M. *Langmuir* **1997**, *13*, 243.

(28) (a) Shneider, T. W.; Buttry, D. A. *J. Am. Chem. Soc.* **1993**, *115*, 12391. (b) Kakiuchi, T.; Usui, H.; Hobaru, D.; Yamamoto, M. *Langmuir* **2002**, *18*, 5231.

In this paper, we describe the first concerted studies of monolayers of thiolipids formed by the Langmuir–Blodgett (LB) and the self-assembly methods. We employ chronocoulometry, a method that has already been used in the study of insoluble films,²⁹ to determine charge densities at the gold electrode covered with LB transferred and self-assembled monolayers of DPTL. When the LB technique is used to deposit dithiols onto the gold surface, the transfer ratio is measured. The packing density of the film at the gold electrode surface is equal to the packing density at the air–solution interface of the Langmuir–Blodgett multiplied by the transfer ratio. The charge number per adsorbed molecule is determined from the ratio of the charge due to adsorbed DPTL to the surface concentration of DPTL. We demonstrate that this number is not constant as assumed in the reductive desorption method (see eq 1) but depends on the electrode potential. We provide a thermodynamic explanation why this charge number has to depend on the electrode potential.

When a monolayer of DPTL is formed by self-assembly from a nonaqueous solution, its packing density is unknown. In this case, the potential-dependent charge numbers per adsorbed molecule, determined for the LB film, are used to calculate the packing density for the self-assembled film using the charge density data measured with the chronocoulometry method. We show that the packing densities determined with this new method are slightly lower than those calculated using the space filling model, and hence, this result is physically reasonable.

2. Experimental Section

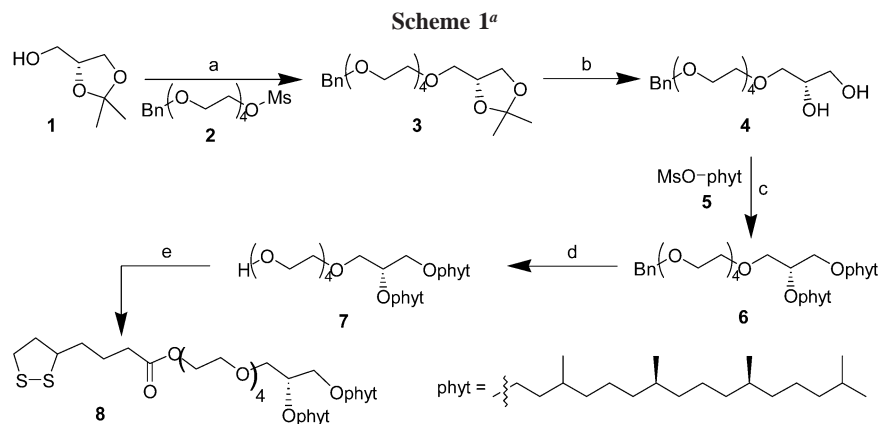
Reagents, Solutions, and Electrode Materials. Gold single crystals, prepared as described in ref 29b, were used as working electrodes for electrochemistry measurements. Before each electrochemical experiment, the working electrode was flame-annealed, cooled first in air and then in water, dried, and transferred into the electrochemical cell to cool in an argon atmosphere. A flame annealed gold coil was used as the counter electrode in all experiments. The reference electrode was an external saturated Ag/AgCl electrode. In this paper, all potentials are referred to the Ag/AgCl scale whose potential versus the saturated calomel electrode SCE was equal to –40 mV.

Prior to all of the experiments, the glassware was cleaned in acid (1:3 mixture of HNO₃ and H₂SO₄) and thoroughly rinsed with Milli-Q and Milli-Q UV plus water. The electrochemical cell was soaked in Milli-Q water overnight and rinsed again prior to the experiment. A 0.1 M NaF (suprapur, EM Industries, Hawthorne, NY) solution was used as the supporting electrolyte for the electrochemical studies. The NaF was cleaned for 30 min in an ozone chamber (UVO cleaner, Jelight, Irvine, CA) before making the solutions. All aqueous solutions were prepared from ultrapure water purified by a Milli-Q UV plus water system (Millipore, Bedford, MA) and having a resistivity 18.2 MΩ cm. All electrolyte solutions were deaerated by purging with argon (BOC Gases, Mississauga, Ontario, Canada) for at least 40 min before starting the experiments, and an argon blanket was maintained over the solution throughout the experiment.

DPTL was dissolved in methanol and deposited onto the Au(111) surface by self-assembly. The self-assembly time was 24 h. This was long enough to form well ordered monolayers. After formation of the SAM, all electrodes were rinsed with methanol and water before introduction to the electrochemical cell.

Independently, the monolayer was transferred from the air–solution interface of a Langmuir trough (KSV LB5000, Finland) onto the gold electrode surface using the Langmuir–Blodgett method by vertically withdrawing the electrode at the speed of 35 mm/min^{–1} at a constant transfer pressure 30 mN m^{–1}. The transfer ratio

(29) (a) Dickertmann, D.; Koppitz, F. D.; Schultze, J.W. *Electrochim. Acta* **1976**, *11*, 967. (b) Richer, J.; Lipkowsky, J. *J. Electrochem. Soc.* **1986**, *133*, 121–128. (c) Bizzotto, D.; Noel, J. J.; Lipkowsky, J. *J. Electroanal. Chem.* **1994**, *369*, 259. (d) Bizzotto, D.; Lipkowsky, J. *J. Electroanal. Chem.* **1996**, *409*, 33. (e) Bizzotto, D.; Lipkowsky, J. *Prog. Colloid Polym. Sci.* **1997**, *103*, 201.



^a Reagents: (a) powdered KOH, DMSO, r.t., 88%; (b) 1 M HCl/MeOH, MeOH, r.t., 78%; (c) powdered KOH, DMSO, r.t., 76%; (d) 10% Pd/C, H₂, EtOAc, 40 °C, 100%; (e) lipoic acid, EDC·HCl, Et₃N, DMAP(cat), CH₂Cl₂, r.t. (14 h) then 40 °C (18 h), 73%.

was 1.0 ± 0.1 . During the vertical withdrawal, the DPTL molecules were oriented with the dithiol headgroup toward the gold surface. The trough was controlled by a computer using KSV LB5000 software. All measurements were carried out at room temperature 20 ± 2 °C.

Synthesis of DPTL. DPTL was synthesized either in the Max Planck Institut für Polymerforschung in Mainz, Germany^{25,30} or at Guelph. The synthesis carried out at Guelph is described in Scheme 1.

1-Phenyl-2,5,8,11-tetraoxatridecan-13-yl methanesulfonate (2). To a flame-dried round-bottom flask was added benzyl tetraethylene glycol³¹ (150 mg, 0.528 mmol), Et₃N (1.8 eq., 95.8 mg, 0.950 mmol, 132 μ L), and 1 mL CH₂Cl₂. The resulting solution was cooled to -30 °C, and then mesyl chloride (1.5 eq, 40.5 mg, 0.792 mmol, 60 μ L) was added dropwise. The reaction was stirred for 3 h (with slowly warming to 0 °C) until the disappearance of starting materials was indicated (TLC). Then aq. NH₄Cl (5 mL) was added, and the organic layer was washed with aq. NH₄Cl, aq. NaHCO₃, and brine and dried over MgSO₄. The solvent was evaporated in vacuo which yielded an oil (191 mg, quantitative) which was used as is. ¹H NMR (400 MHz, CDCl₃), δ : 7.35–7.27 (m, 5H), 4.56 (s, 2H), 4.37–4.35 (m, 2H), 3.76–3.74 (m, 2H), 3.68–3.61 (m, 12H), 3.06 (s, 3H); ¹³C (100 MHz, CDCl₃), δ : 138.02, 128.11, 127.48, 127.35, 72.92, 70.35, 70.25, 69.18, 68.71, 45.85, 37.39; IR (neat) cm⁻¹: 3029, 2870, 1454, 1352, 1249, 1175, 1110, 1019; MS(EI), m/z (%): 362 (M⁺, 3), 167 (13), 134 (7), 123 (86), 106 (10), 91 (100), 79 (18); MS(HREI): C₁₆H₂₆O₇S Calcd 362.1399. Found 362.1398.

(4R)-2,2-Dimethyl-4-(15-phenyl-2,5,8,11,14-pentaoxapentadecan-1-yl)-1,3-dioxolane (3). To a flame-dried round-bottom flask was added powdered KOH (2.5 eq, 1.27 g, 22.6 mmol) and dry DMSO (40 mL). The resulting suspension was stirred for 1 h at r.t. Then a solution of **2** (1.0 eq., 3.27 g, 9.03 mmol) and **1** (1.0 eq, 1.19 g, 9.03 mmol) ($[\alpha]_D^{24} = +15.0$ (neat), $[\alpha]_D^{20} = +15.2$, ref 32) in dry DMSO (15 mL) was added. The reaction was stirred at r.t for 24 h and then warmed to 40 °C for 18 h. Water (150 mL) was added, and the aqueous phase was extracted with EtOAc (4 \times 100 mL) where the combined extracts were washed with water (6 \times 100 mL) and brine and dried over MgSO₄. The solvent was evaporated in vacuo yielding **3** as a yellow oil (3.13 g, 87%), which was used as is for additional reactions. A small sample was purified by flash chromatography (1:1 EtOAc:hexanes, $R_f = 0.50$ EtOAc) for spectroscopic data. ¹H NMR (400 MHz, CDCl₃), δ : 7.36–7.27 (m, 5H), 4.57 (s, 2H), 4.31–4.25 (m, 1H), 4.04 (dd, $J = 8.3, 6.4$ Hz, 1H), 3.72 (dd, $J = 8.3, 6.4$ Hz, 1H), 3.58 (dd, $J = 10.0, 5.7$ Hz, 1H), 3.50 (dd, $J = 10.0, 5.5$ Hz, 1H), 1.41 (s, 3H), 1.35 (s, 3H); ¹³C (100 MHz, CDCl₃), δ : 137.92, 127.94, 127.29, 127.16, 108.87, 74.31, 72.77, 71.92, 70.56, 70.23, 69.05, 66.39, 26.42, 25.05; IR (neat)

cm⁻¹: 3063, 3030, 2985, 2868, 1454, 1380, 1370, 1351, 1291, 1253, 1213, 1104; MS(EI), m/z (%): 398 (M⁺, 3), 383 (27), 133 (16), 101 (58), 91 (100); $[\alpha]_D^{24} = +6.04$ ($c = 8.89$, CH₂Cl₂); Elemental Analysis for C₂₁H₃₄O₇: Calcd C 63.30, H 8.60%. Found C 63.12, H 8.61%.

(16S)-1-Phenyl-2,5,8,11,14-pentaoxaheptadecane-16,17-diol (4). To a round-bottom flask was added **5** (2.14 g, 5.37 mmol) and 45 mL of MeOH. Then a 1 M solution of HCl in MeOH 47.5 mL (prepared fresh from concentrated HCl and MeOH) and the reaction was stirred overnight. The solvent was evaporated in vacuo yielding **4** as an oil (quantitative by mass), which was chromatographed (flash conditions, EtOAc to 25:75 EtOH:EtOAc, $R_f = 0.24$ (9:1) EtOAc:EtOH) yielding **4** as an oil (1.41 g, 78%). ¹H NMR (400 MHz, CDCl₃), δ : 7.35–7.27 (m, 5H), 4.57 (s, 2H), 3.87–3.83 (m, 1H), 3.72–3.54 (m, 20 H), 2.44 (br s, 2H); ¹³C (100 MHz, CDCl₃), δ : 138.08, 128.26, 127.67, 127.51, 73.12, 72.77, 70.53, 70.48, 70.40, 69.28, 63.73; IR (neat) cm⁻¹: 3419 (br), 3031, 2871, 1454, 1351, 1250, 1104; $[\alpha]_D^{24} = -2.75$ ($c = 2.19$, CH₂Cl₂); Elemental Analysis for C₁₈H₃₀O₇: Calcd C 60.32, H 8.44%. Found C 60.11, H 8.35%.

Phytanol Methanesulfonate (5). To a flame-dried round-bottom flask was added phytanol³³ (prepared from phytol, Raney Ni, H₂, EtOH, 40 °C, 3d, 100%) (6.10 g, 20.4 mmol), 20 mL of CH₂Cl₂, and Et₃N (1.8 eq., 3.72 g, 5.13 mL, 36.8 mmol), and the mixture was cooled to 0 °C. Then mesyl chloride (1.5 eq., 3.51 g, 2.37 mL, 30.6 mmol) was added over 5 min. The reaction was stirred for 3 h until starting material consumption was detected by TLC. Then aq. NH₄Cl (40 mL) was added and the organic layer was washed with aq. NH₄Cl, water, aq. NaHCO₃, water, and brine and was dried over MgSO₄. The solvent was evaporated in vacuo yielding **5** as an oil (7.68 g, quantitative). ¹H NMR (400 MHz, CDCl₃), δ : 4.25–4.21 (m, 2H), 2.97 (s, 3H), 1.79–1.73 (m, 1H), 1.58–1.47 (m, 3H), 1.40–1.05 (m, 20H), 0.89 (d, $J = 6.2$ Hz, 3H), 0.86 (br d, $J = 6.8$ Hz, 6H), 0.84 (v br d, $J = 6.7$ Hz, 6H); ¹³C (100 MHz, CDCl₃), δ : 68.52, 39.26, 37.32, 37.28, 37.22, 37.19, 37.17, 37.09, 37.01, 36.98, 35.94, 35.86, 32.65, 29.26, 27.86, 24.70, 24.36, 24.13, 22.63, 22.54, 19.65, 19.52, 19.20, 19.13; IR (neat) cm⁻¹: 2955, 2927, 2869, 1464, 1357, 1177; MS(EI), m/z (%): 280 (26), 196 (17), 140 (36), 126 (54), 125 (69), 111 (55), 97 (57), 85 (40), 83 (71), 71 (78), 70 (70), 69 (96), 57 (100), 55 (78); MS(CI), m/z (%): 394 (M+NH₃, 100); $[\alpha]_D^{24} = +0.0323$ ($c = 18.5$, CH₂Cl₂); Elemental Analysis for C₂₁H₄₄O₃S: Calcd C 66.97, H 11.78%. Found C 66.71, H 11.55%.

(16S,25R,29R)-1-Phenyl-21,25,29,33-tetramethyl-16-[[[(7R,11R)-3,7,11,15-tetramethylhexadecyl]oxy]-2,5,8,11,14,18-hexaoxatetra-triacontane (6). To a flame-dried round-bottom flask was added powdered KOH (5 e.q., 1.04 g, 18.6 mmol) and dry DMSO (10 mL). The reaction was stirred for 10 min and then cooled in an ice bath, and a solution of **4** (1 e.q., 1.33 g, 3.72 mmol) and **5** (3 e.q., 4.20 g, 11.2 mmol) in dry DMSO (10 mL) was added over 2 min. The ice bath was removed and the reaction was stirred overnight at r.t.

(30) Schiller, S. M.; Naumann, R.; Lovejoy, K.; Kunz, H.; Knoll, W. *Angew. Chem., Int. Ed.* **2003**, *42* (2), 208.

(31) Renkes, T.; Schafer, H. J.; Siemens, P. M.; Neumann, E. *Angew. Chem., Int. Ed.* **2000**, *39*, 2512.

(32) Eibl, H. *Chem. Phys. Lipids* **1981**, *28*, 1.

(33) Bendavid, A.; Burns, C. J.; Field, L. D.; Hashimoto, K.; Ridley, D. D.; Sandanayake, K. R. A. S.; Wieczorek, L. *J. Org. Chem.* **2001**, *66*, 3709.

and then heated to 40 °C for 3 days. Water (70 mL) was added, and the resulting solution was extracted with EtOAc (4 × 50 mL) and the combined organic layers were washed with water (6 × 100 mL) and brine (50 mL), dried with MgSO₄, and evaporated in vacuo yielding **6** as an oil. Flash chromatography (1:4 EtOAc:hexanes, $R_f = 0.25$ (1:4) EtOAc:hexanes) yielded **6** as a light yellow oil (3.42 g, 76%). ¹H NMR (400 MHz, CDCl₃), δ: 7.34–7.27 (m, 5H), 4.57 (s, 2H), 3.69–3.41 (m, 25H), 1.64–1.47 (m, 8H), 1.38–1.01 (m, 44H), 0.86 (br d, $J = 6.6$ Hz, 18H), 0.84 (v br d, $J = 6.6$ Hz, 12H); ¹³C (100 MHz, CDCl₃), δ: 138.04, 128.05, 127.41, 127.27, 77.70, 72.96, 71.22, 70.71, 70.65, 70.42, 70.33, 69.62, 69.21, 68.56, 39.14, 37.28, 37.22, 37.16, 37.06, 36.96, 36.88, 36.53, 36.45, 32.53, 29.62, 29.53, 27.72, 24.57, 24.24, 24.14, 22.52, 22.42, 19.55, 19.48, 19.41; IR (neat) cm⁻¹: 3064, 3030, 2953, 2926, 2868, 1463, 1377, 1366, 1249, 1114, 1044; MS(TOF ES), m/z (%): 648 (71), 513 (25), 433 (100); MS(HRCl), m/z (%): (M+NH₄) Calcd 936.8595. Found 936.8545; $[\alpha]_D^{24} = -0.301$ ($c = 3.42$, CH₂Cl₂).

(14*S*,23*R*,27*R*)-19,23,27,31-Tetramethyl-14-[[[(7*R*,11*R*)-3,7,11,15-tetramethylhexadecyl]oxy]-3,6,9,12,16-pentaoxadotriacontan-1-ol (**7**). To a round-bottom flask was added **6** (2.33 g, 2.53 mmol), 40 mL of EtOAc, and 10% Pd/C (400 mg), and the solution was degassed (3×). Then hydrogen was introduced under balloon pressure (15–16 psi) and the reaction was warmed to 40 °C for 24 h. The reaction was filtered through Celite and washed with EtOAc thoroughly. The solvent was evaporated in vacuo yielding **7** as an oil. Flash chromatography (1:1 EtOAc:hexanes, $R_f = 0.26$ (1:1) EtOAc:hexanes) yielded **7** as an oil (2.10 g, quantitative). ¹H NMR (400 MHz, CDCl₃), δ: 3.74–3.71 (m, 2H), 3.69–3.44 (m, 23H), 2.0 (br s, 1H, OH), 1.66–1.47 (m, 6H), 1.39–0.98 (m, 42H), 0.86 (br d, $J = 6.7$ Hz, 18H), 0.85 (v br d, $J = 6.7$ Hz, 12H); ¹³C (100 MHz, CDCl₃), δ: 77.78, 72.43, 71.32, 70.81, 70.75, 70.51, 70.49, 70.44, 70.25, 69.80, 68.73, 61.55, 39.24, 37.38, 37.33, 37.27, 37.16, 37.06, 36.97, 36.62, 36.54, 32.83, 32.65, 29.75, 29.67, 27.83, 24.67, 24.35, 24.25, 22.61, 22.52, 19.64, 19.57, 19.50; IR (neat) cm⁻¹: 3466 (br), 2954, 2926, 2868, 1463, 1377, 1366, 1351, 1118; MS(TOF ES), m/z (%): 851 (M+Na, 3), 648 (37), 433 (100), 383 (5); $[\alpha]_D^{24} = -0.331$ ($c = 2.93$, CH₂Cl₂); Elemental Analysis for C₅₁H₁₀₄O₇: Calcd C 73.86, H 12.64%. Found C 73.64, H 12.76%.

(3*R*)-(14*S*,23*R*,27*R*)-19,23,27,31-Tetramethyl-14-[[[(7*R*,11*R*)-3,7,11,15-tetramethylhexadecyl]oxy]-3,6,9,12,16-pentaoxadotriacont-1-yl ester-1,2-dithiolane-3-pentanoate (**8**). To a flame-dried round-bottom flask was added lipoic acid (1.27 eq., 518 mg, 2.5 mmol), EDC·HCl (1.4 eq., 498 mg, 2.56 mmol), DMAP (0.075 eq., 23 mg, 0.188 mmol), and 17 mL of dry CH₂Cl₂. The resulting mixture was stirred vigorously, and then a solution of **7** (1.0 eq., 1.68 g, 2.02 mmol) and Et₃N (1.5 eq., 280 mg, 2.76 mmol, 385 μL) in dry CH₂Cl₂ (12 mL) was added. The reaction mixture was stirred for 14 h at r.t. and then warmed to 40 °C for 18 h. Then aq. NH₄Cl (30 mL) and water (40 mL) were added, and the mixture was extracted with CH₂Cl₂ (3 × 30 mL). The combined layers were washed with aq. NH₄Cl (30 mL), water (30 mL), aq. NaHCO₃ (30 mL), water (30 mL), and brine. The organic layer was dried over MgSO₄ and evaporated in vacuo to yield **8** as a yellow oil. Flash chromatography (1:4 EtOAc:hexanes, $R_f = 0.22$ (1:4) EtOAc:hexanes) yielded **8** as a yellow oil (1.50 g, 73%). ¹H NMR (400 MHz, CDCl₃), δ: 4.24–4.21 (m, 2H), 3.70–3.68 (m, 2H), 3.66–3.42 (m, 21H), 3.21–3.08 (m, 2H), 2.46 (app sextet, $J = 6.3$ Hz, 1H), 2.35 (t, 7.4 Hz, 2H), 1.91 (app sextet, $J = 6.7$ Hz, 1H), 1.73–0.98 (m, 55H), 0.86 (br d, $J = 6.7$ Hz, 18H), 0.84 (v br d, $J = 6.7$ Hz, 12H); ¹³C (100 MHz, CDCl₃), δ: 173.05, 77.70, 71.25, 70.69, 70.46, 70.41, 70.36, 69.68, 68.96, 68.61, 63.20, 56.04, 2.73, 39.16, 38.23, 37.24, 37.18, 37.07, 36.98, 36.90, 36.55, 36.46, 34.39, 33.69, 32.56, 29.66, 29.57, 28.50, 27.75, 24.59, 24.40, 24.27, 24.16, 22.55, 22.45, 19.58, 19.51; IR (neat) cm⁻¹: 2954, 2927, 2867, 1739, 1462, 1377, 1366, 1351, 1325, 1301, 1250, 1119; MS(TOF ES), m/z (%): 1018 (M+, 19), 649 (97), 513 (23), 433 (100); $[\alpha]_D^{24} = -0.663$ ($c = 1.65$, CH₂Cl₂); Elemental Analysis for C₅₉H₁₁₆O₈S₂: Calcd C 69.93, H 11.49%. Found C 69.76, H 11.23%.

Electrochemical Measurements and Instrumentation. Electrochemical measurements were carried out in an all-glass three electrode cell using the working electrode in the hanging meniscus

configuration.^{29a} Differential capacitance measurements were used to check the cleanliness of the electrode and the electrolyte solution. To determine the differential capacitance curves, an AC perturbation of 25 Hz frequency and 5mV rms amplitude was superimposed onto a 5 mV/s voltage ramp. Electrochemical experiments were performed using a computer-controlled system, consisting of a HEKA potentiostat/galvanostat PG490, a scan generator ESG 310 (HEKA, Lambrecht/Pfalz, Germany), and a 7265 DSP lock-in amplifier (EG & G Instruments, Cypress, CA). Data acquisition was performed via a plug-in acquisition board (NI-6052E, Austin, Texas) and in-house software. A series RC equivalent circuit was employed to calculate the differential capacity curves from the in-phase and the out-of-phase components of the AC current.

The capacity curves give a first insight into the electrochemical behavior of the system. In addition, chronocoulometry was employed as a potentiostatic method to determine the charge density at the electrode surface. In this series of experiments, the Au(111) electrode was held at a base potential $E_b = +200$ mV for 120 s. Then the potential was stepped to a variable value of interest starting from the most positive potential (+400 mV) E_f , and kept constant for another 120 s. To desorb the thiolipid from the electrode surface, the potential was stepped to $E_{des} = -1200$ mV. The current transient corresponding to desorption of DPTL was measured during 0.15 s. The potential was then stepped back to the base value of $E_b = +200$ mV. Integration of the current transients gives the difference between charge densities at potentials E_c and E_{des} . The charge density curves measured with and without DPTL merged at the most negative potentials. The absolute charge densities for the electrode without the surfactant can be calculated knowing the potential of zero charge, $E_{pzc} = +300$ mV vs Ag/AgCl, determined independently. The absolute charge densities for the electrode covered with DPTL were calculated assuming that at $E = -1.2$ V the charge density for the electrode initially covered by DPTL is equal to the charge density of the electrode without DPTL. The data processing is described in detail in ref 29b–e. The electrolyte solution was stirred during the chronocoulometry measurements, even though the bulk electrolyte solution did not contain any surfactant molecules, to ensure that there are no differences between the composition of the electrolyte near the surface and in the bulk. The SAM was formed on the Au(111) electrode prior to each experiment.

3. Results and Discussion

DPTL Monolayer at the Air–Solution Interface and LB Transfer. A few drops of DPTL solution in chloroform (Fisher 99.9%) were injected onto the water surface of the Langmuir trough. The solvent was allowed to evaporate, and the compression isotherm was recorded. Figure 2 depicts the surface pressure (Π)–molecular area isotherm of DPTL at the air–water interface. The first compression cycle starts at ~223 Å² per molecule, and the collapse of the film is observed at a molecular area of ~100 Å² and a pressure of ~34 mN m⁻¹. The shape of the compression isotherm is characteristic of a liquid expanded monolayer. When the first decompression of the film is recorded, a significant hysteresis is observed. The decompression curve is steeper and is completed at a molecular area ~190 Å². The hysteresis is observed on every subsequent compression–decompression cycle. While the collapse pressure remains constant at 34 mN m⁻¹, the mean molecular area at the collapse point and the molecular area at the completion of the decompression progressively decrease with the number of compression–decompression cycles. Figure 2 shows that after four compression–decompression cycles the collapse point has shifted to ~80 Å² and the last decompression was completed at ~155 Å². The inset to Figure 2 shows that the hysteresis is also observed when the film is compressed only to the film pressure 30 mN m⁻¹ which is below the critical point. Therefore, the hysteresis is not due to a loss of the molecules due to bilayer formation after the collapse point.

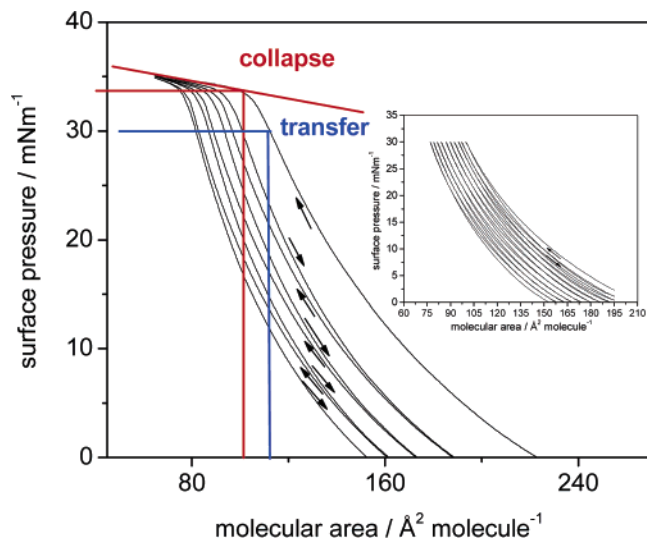


Figure 2. Compression isotherms for DPTL on a pure water subphase recorded at a compression rate of 10 mN mm^{-1} . Inset similar compression isotherms as in the main section with the highest film pressure below the collapse point.

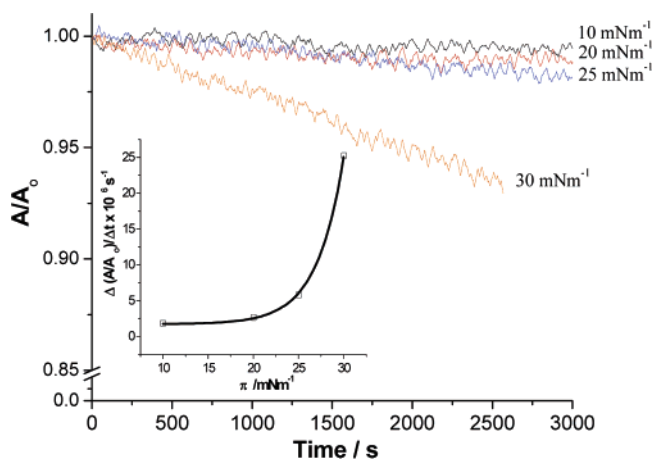


Figure 3. Change of the normalized the area of the film covered surface as a function of time recorded during the isobaric creep experiment, A_0 and A are the initial area of the film covered surface and the area at a given time t . Inset shows slopes of the isobaric plots as a function of the film pressure.

Additional isobaric creep experiments were performed in order to understand the nature of the hysteresis. The monolayer of DPTL was compressed to a specified pressure which was then kept constant during ~ 3000 s and the change in the area of the trough covered by the film was recorded. Figure 3 plots the ratio A/A_0 as a function of time for selected film pressures, where A_0 and A are the initial area of the film covered surface and the area at a given time t . For pressures lower than 15 mN m^{-1} , the creep was very small. At higher pressures, a significant creep was observed. Since A varied approximately linearly with time, the creep can be represented by the slope of the A/A_0 versus time plots. The values of $\Delta(A/A_0)/\Delta t$ are plotted as a function of the surface pressure in the inset to Figure 3. The result shows that the creep becomes pronounced for film pressures higher than 15 mN m^{-1} . Indeed, no hysteresis on the compression isotherms was observed if the compression was performed at film pressures lower than 15 mN m^{-1} .

The properties of the monolayer of DPTL are consistent with the behavior of monolayers of poly(ethylene oxide) lipopolymers³⁴ and poly(styrene)–poly(ethylene oxide) diblock copolymers.^{35,36} At low film pressures, the poly(ethylene oxide) chains

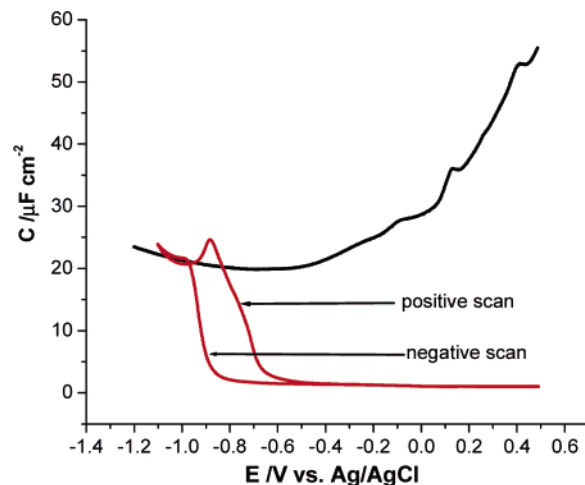


Figure 4. Differential capacity versus potential curves of a Au(111) electrode in 0.1 M NaF for the film-free interface (black line) and the interface covered with SAM adsorbed for 24 h DPTL (red lines). For the SAM covered electrode the curves were recorded starting at $E = 0.45 \text{ V (SCE)}$ and by applying a 5 mV s^{-1} voltage scan in the negative direction. The direction of the voltage scan was reversed at $E = -1.1 \text{ V (SCE)}$; arrows indicate the curves recorded during the negative and positive voltage scan. To measure the capacity, a 5 mV rms ac perturbation of 25 Hz was superimposed onto the voltage ramp; a simple RC circuit was used to calculate the capacity from the impedance data.

are oriented parallel to the surface and the adsorbed molecule has a “pancake” shape. At film pressure $\sim 10 \text{ mN m}^{-1}$ the poly(ethylene oxide) chains become soluble in the aqueous subphase and the adsorbed molecule adopts a “mushroom” structure. At higher film pressures, the poly(ethylene oxide) chains have a tendency to coil. They become hydrophobic and can be densely packed. The adsorbed molecule undergoes a further conformational change to the “brush” structure.

A progressive transformation of adsorbed molecules from the “pancake” to “mushroom” and from “mushroom” to “brush” conformations can explain the hysteresis observed in Figure 2. The high cohesion energy between poly(ethylene glycol) chains in the “brush” conformation induces association and local ordering of DPTL molecules. In addition, an entanglement of the chains may take place at high film pressures. The association and the chain entanglement prevent an easy reformation of the adsorbed molecules into the “pancake” state during the decompression cycle.

To ensure reproducibility of the state of the monolayer, the LB transfer was performed at 30 mN m^{-1} (molecular area of 112 \AA^2), during the first compression of the film. For each transfer, a new DPTL film was spread onto the air–water interface, compressed until the desired pressure of 30 mN m^{-1} was reached, and then transferred onto the electrode. Using this approach, the molecular area remained the same for each transfer of the film.

Differential Capacity. The behavior of the DPTL coated electrode was initially characterized with the help of differential capacity. Figure 4 shows the potential driven transformations of a DPTL monolayer adsorbed on the Au(111) surface observed by recording the differential capacity curve. The black line depicts the capacity versus potential curve for the film free Au(111) electrode, the red curves display the capacity versus potential

(34) Baekmark, T. R.; Elender, G.; Lasic, D. D.; Sackmann, E. *Langmuir* **1995**, *11*, 3975–3987.

(35) Goncalves da Silva, A. M.; Filipe, E. J. M.; d’Oliveira, J. M. R.; Martinho, J. M. G. *Langmuir* **1996**, *12*, 6547–6553.

(36) Logan, J. F.; Masse, P.; Gnanou, Y.; Taton, D.; Duran, R. S. *Langmuir* **2005**, *21*, 7380–7389.

plots of the Au(111) electrode covered with a monolayer of DPTL self-assembled during 24 h from a solution of DPTL in methanol. To record the capacity curve a slow voltage scan was applied to a DPTL covered electrode, brought in contact with the electrolyte solution at +500 mV. The differential capacity curve shows that DPTL is stable over a wide potential range from -650 to $+500$ mV. In the potential range between -400 and $+400$ mV, the capacity attains a minimum value of $0.81 \mu\text{F cm}^{-2}$. At potentials < -800 mV the film is detached from the surface and the capacity increases up to a value of $22 \mu\text{F cm}^{-2}$ and essentially merges with the curve recorded at the DPTL free electrode.

When the direction of the voltage scan is reversed and the electrode potential moves back to more positive values, a readsorption of the thiolipid molecules is observed. This behavior indicates that in the desorbed state the DPTL molecules remain close to the electrode surface, most likely in the form of aggregates, in good agreement with the behavior of other insoluble films of amphiphilic molecules.^{29c-e} The hysteresis on the differential capacity curves shows that the kinetics of the desorption and the respreading of the film are slow.

For the film self-assembled during 24 h, no difference in the minimum value of the capacity measured in the first (desorption) and the second (readsorption) potential scan was observed. Apparently, the structure of the organic film does not change after readsorption of the DPTL molecules. However, when the self-assembled layers were formed using shorter adsorption (self-assembly) times somewhat higher values of the minimum capacity were observed. In addition, the capacity measured in the readsorption half cycle was always somewhat higher than the capacity measured in the first desorption cycle.

We emphasize that the capacity curves have been calculated from a single frequency impedance measurement, assuming that the interface may be represented by a simple RC circuit. They are used for a qualitative characterization of the DPTL covered electrode only. A quantitative analysis of the film covered interface is based on the charge density measurements described below.

Charge Potential Curves. Figure 5 shows the charge potential plots determined from chronocoulometric experiments. The black line (and black squares) marks the curve determined for the Au(111) electrode in the absence of DPTL. The red lines (red squares or circles) depict the charge potential plots determined for the electrode covered by the self-assembled DPTL film. The blue line and squares show the curve determined for the electrode covered by DPTL film transferred from the air–solution interface using the LB method.

Figure 5b shows the program of potential pulses used to determine the charge-potential curves marked as black, red, and blue squares. To acquire these data, the potential was held for 120 s at a base potential value 0.2 V for a period of 120 s, and then it was changed to the sample potential for another 120 s. The sample potential is plotted on the coordinate axis in Figure 5a. Finally, the potential was stepped to desorption potential -1.2 V, and the charge difference between the sample potential and desorption potential was measured. The base potential was applied to allow the film to recover at the same conditions from the large pulse applied to the desorption potential. Hydrogen evolution takes place at $E = -1.2$ V. To verify that the hydrogen evolution reaction does not affect the measured charge densities, a program of potential pulses shown in Figure 5c was employed. For the electrode covered by the self-assembled film, charge densities determined using this program are shown as open red circles in Figure 5a. In this case, the base potential was -0.4 V and the potential was stepped between a value plotted on the

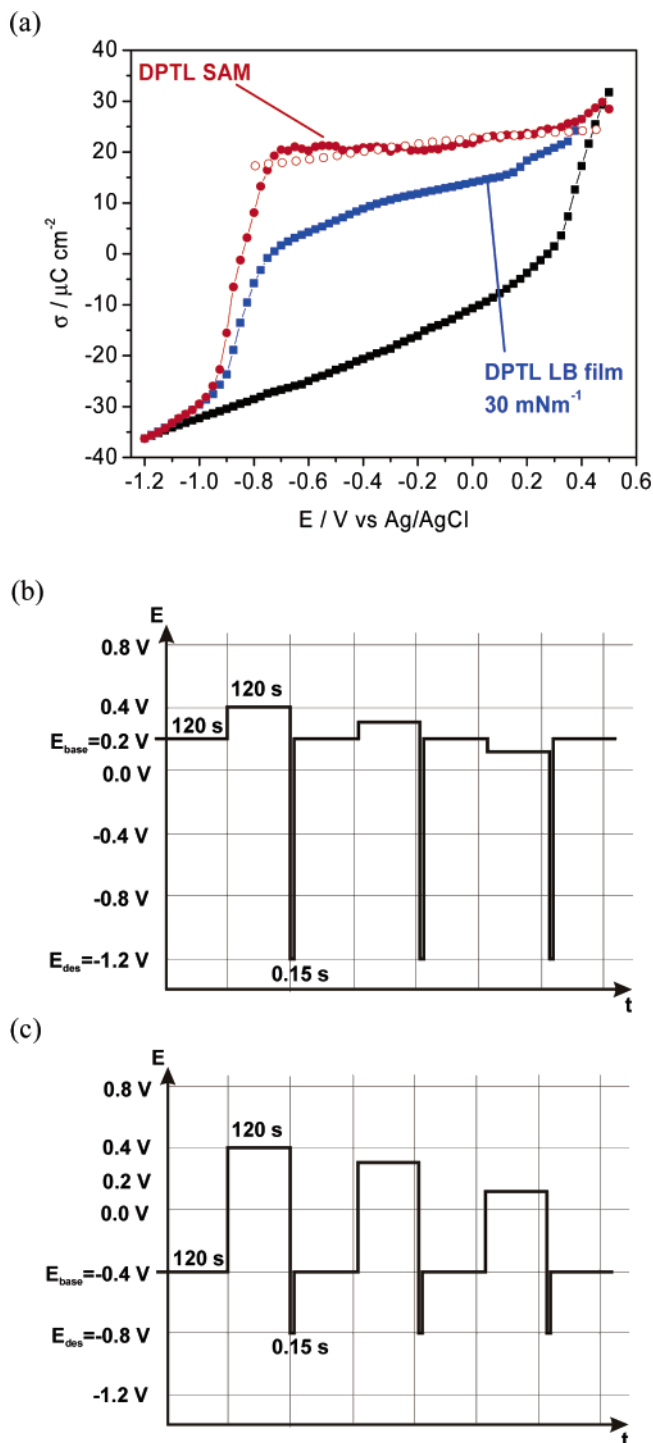


Figure 5. (a) Charge density σ_M versus potential curves for the Au(111) electrode in 0.1 M NaF without DPTL (filled black squares) and with DPTL adsorbed on the surface by self-assembly for 24 h (red circles) or LB transfer at 30 mN m^{-1} (blue squares); for detailed explanations see text. (b) Sequence of the potential steps for the acquisition of the data marked in (a) with filled symbols; $E_{\text{base}} = +0.2$ V, E_f changes from $+0.4$ V down to -1.175 V, $E_{\text{des}} = -1.2$ V. (c) Sequence of potential steps for the data shown in (a) shown as empty red circles; $E_{\text{base}} = -0.4$ V, E_f changes from $+0.4$ V down to $+0.1$ V, $E_{\text{des}} = -0.8$ V.

coordinate in Figure 5a and $E = -0.8$ V. Only one potential step from $E = -0.8$ to -1.2 V was performed to determine the absolute charge densities for this series of measurements. In contrast to the data plotted as red squares, where each point represents consecutive desorption and readsorption of the film, the data plotted as open red circles correspond to the case where the film

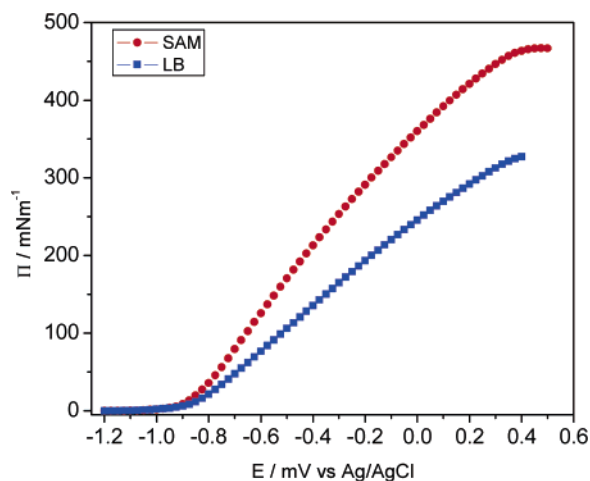


Figure 6. Surface pressure $\Pi = \int_{E=-1200}^E \Delta\sigma \, dE$ versus potential E plots calculated from the charge density curves; (red symbols) for the self-assembled film; blue symbols for the LB-transferred film.

was desorbed only once at the end of the experiment. The differences between the two series of measurements are small indicating that the multiple desorption–readsorption cycles did not affect the integrity of the film.

The charge density curves for the DPTL covered electrode merge with the curve for the film free electrode at the most negative potentials indicating that the film is totally desorbed from the gold surface. When the potential is moved in the positive direction a large step corresponding to the desorption–adsorption of DPTL can be seen on the curves for the film covered electrode. The step is much higher for the self-assembled than for the LB transferred film, indicating that the self-assembled film is more compact. The curves for the self-assembled film show a plateau in the potential range between -700 and $+400$ mV. A very small slope at this plateau is indicative of a very low capacity of this film. In contrast, the slope at the “plateau” of the charge density curve corresponding to LB transferred film is much higher indicating a higher capacity of that film. This behavior confirms that the LB film is less compact than the self-assembled film.

The area between the charge density curves for the supporting electrolyte and the electrode covered by the DPTL monolayer corresponds to the surface pressure of the adsorbed film which can be calculated using the following equation:^{29b–e}

$$\Pi = \gamma_0 - \gamma = \int_{E=-1200}^E \sigma_M \, dE - \int_{E=-1200}^E \sigma_{M_0} \, dE = \int_{E=-1200}^E \Delta\sigma_M \, dE \quad (2)$$

where γ_0 and γ are the surface energies and σ_M and σ_{M_0} are the charge densities in the absence and in the presence of a surfactant monolayer on the surface and $\Delta\sigma_M = \sigma_M - \sigma_{M_0}$. The surface pressure versus potential curves for SAMs and LB films are shown in Figure 6. They are approximately bell shaped with the maximum observed at ~ 0.5 V. This is the potential of the maximum adsorption of DPTL at the Au(111) electrode surface (E_{\max}). The pressure at E_{\max} differs significantly between the self-assembled and LB transferred films. The highest pressure of $\Pi = 467$ mN m⁻¹ is calculated for the self-assembled film. The LB film shows a maximum pressure of $\Pi = 327$ mN m⁻¹. This difference points to a lower packing density in the LB transferred film. The surface pressures of the DPTL films on the electrode surface are more than order of magnitude higher than the pressure of the film measured at the air–water interface, which collapses at $\Pi \approx 34$ mN m⁻¹ and the area per molecule

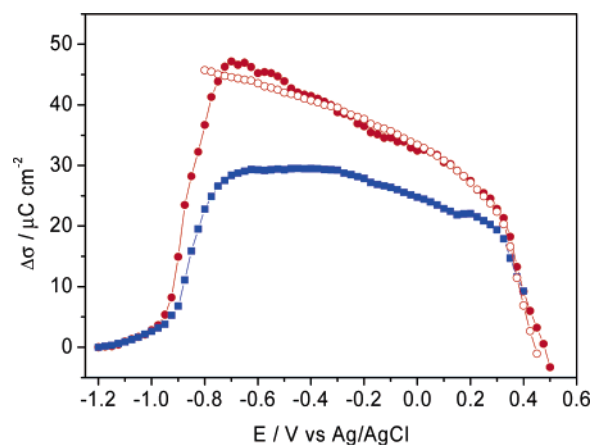


Figure 7. Charge density difference $\Delta\sigma = \sigma_M - \sigma_{M_0}$ versus potential curves for the Au(111) electrode in 0.1 M NaF covered by DPTL film; (filled red circles) SAM, charge densities acquired using the potential step program described in Figure 5b; (empty red circles) SAM, charge densities acquired using the potential step program described in Figure 5c; (blue squares) film transferred using the LB technique at 30 mN m⁻¹, using the potential step program described in Figure 5b.

of ~ 100 Å² (see Figure 2). The difference between the film pressure at the gold–solution and the air–solution interfaces is due to the formation of a strong gold–thiol chemisorption bond.

Charge Numbers per Adsorbed Molecule and Packing Density in the Self-Assembled Monolayer. Figure 7 plots the difference between the charge density corresponding to the film free electrode (black line in Figure 4a) and the charge density for the electrode covered by the self-assembled (red symbols) and LB transferred (blue symbols) films. These curves display a change of the charge density due to adsorption of DPTL molecules. Their sign is positive indicating that a positive charge flows to the electrode when DPTL adsorbs at the gold surface. The change of charge displays a maximum at $E \sim -0.8$ V and drops to zero at $E \sim 0.5$ V at the potential of the maximum adsorption of the film.

The LB film was transferred (with a transfer ratio of 1 ± 0.1) onto the electrode surface at an air–solution film pressure of $\Pi = 30$ mN m⁻¹, corresponding to a packing density of DPTL molecules at the surface of the Langmuir trough $\Gamma = 1.48 \times 10^{-10}$ mol cm⁻². Consequently, the packing density in LB film at the electrode surface was $1.5 \pm 0.15 \times 10^{-10}$ mol cm⁻². Knowing the packing density for the LB film, one may calculate the charge number l per adsorbed DPTL molecule employing the equation

$$l = -\frac{1}{F} \left(\frac{\Delta\sigma}{\Delta\Gamma} \right)_E = -\frac{1}{\Gamma} \left(\frac{\partial\Pi}{\partial E} \right)_\Gamma \quad (3)$$

It is useful to stress that this quantity is an integral form of the charge number at a constant electrode potential defined as $l = -1/F(\partial\sigma_M/\partial\Gamma)_E$ and known also as the “electrosorption valency”.³⁷

The charge numbers calculated with the help of eq 3 are plotted against potential in Figure 8. The calculations have been restricted to $E > -0.7$ V where we can reasonably assume that all DPTL molecules transferred by the LB method remain at the electrode surface. The charge number clearly depends on the electrode potential. Within a narrow potential range between -0.7 and -0.3 V the charge number is equal to ~ -2 . However, at $E > -0.3$ V, the absolute value of the charge number drops down significantly. Extrapolation of these data gives $l = 0$ at $E \sim 0.5$

(37) Trasatti, S.; Parsons, R. *J. Electroanal. Chem.* **1986**, *205*, 359.

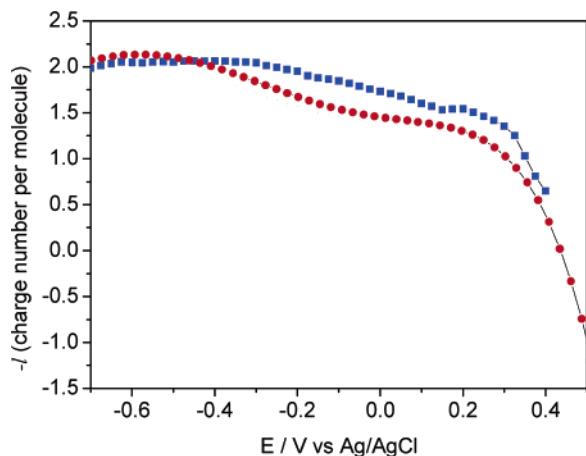


Figure 8. Charge number per adsorbed molecule for the LB layer (blue squares) and calculated with the help of eq 16 (red symbols).

V. This result is consistent with experiments performed by Kryszinski et al.³⁸ involving a potentiostatic LB transfer of octadecanethiol onto a gold electrode. Kryszinski et al.³⁸ were the first to report that the charge per adsorbed thiol molecule is less than the number of electrons involved in the surface redox reaction and discussed this result in terms of a “partial electron transfer”. We will provide a different interpretation of the “partial charge number”. It is also consistent with the work by Schneider and Buttry,^{28a} who reported partial values of the electroadsorption valency for thiols at a gold electrode surface.

Assuming that the charge number per adsorbed DPTL molecule is the same in the LB and the self-assembled film, one can use l values from Figure 8 and the $\Delta\sigma$ data from Figure 7 to calculate the packing densities for the self-assembled film. The packing densities are plotted as a function of potential in Figure 9a. Their values are equal to $2.2 \pm 0.2 \times 10^{-10}$ mol cm⁻². Figure 9b plots corresponding areas per molecule which are equal to 85 ± 9 Å². The 10% error is due to the uncertainty of the LB transfer procedure. The weak potential dependence of the packing density and area per molecule may reflect small systematic errors in the charge density measurements. It may also reflect a slightly different potential dependence of l for the LB and the self-assembled films. The area per molecule needed to accommodate two phytanyl chains is equal to 65 Å².²⁵ Our number is about 25% higher than this limiting value which is physically reasonable.

At this point, we can compare packing densities determined by combined chronocoulometric experiments on the LB and the self-assembled films with the packing densities calculated by the “reductive desorption” method. In the latter method, one measures the charge difference between a potential at which a thiol forms a monolayer and a potential at which the film is desorbed. Usually, this charge is determined by integration of a cyclic voltammogram. This charge is then divided by the number of electrons transferred to the thiol (in the present case 2) and the Faraday constant. When applied to the charge densities determined by chronocoulometry, the “reductive desorption” method is equivalent to calculation of the surface concentration of the self-assembled thiol using the formula

$$\Gamma = \frac{\sigma_M(E) - \sigma_M(-1.2V)}{2F} \quad (4)$$

where $\sigma_M(E)$ is the charge density at a potential at which the

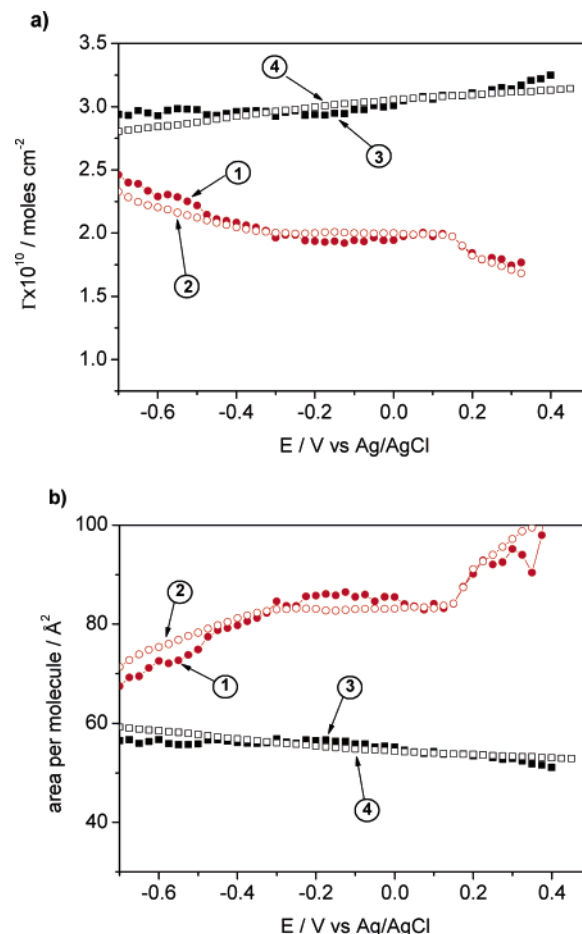


Figure 9. (a) Surface concentration versus potential plots, for a monolayer of DPTL self-assembled at a gold electrode surface. Curves (1) and (2): Surface concentration calculated from $\Delta\sigma_M$ data shown in Figure 7 and charge numbers l given in Figure 8. Curves (3) and (4): Surface concentration calculated from the reductive desorption model and eq 4. Curves (1) and (3) correspond to the charge density data acquired using the potential step program described in Figure 5b. Curves (2) and (4) correspond to the charge densities determined using the potential step program described in Figure 5c. (b and a) Area per adsorbed DPTL molecule versus potential plots, for a monolayer of DPTL self-assembled at a gold electrode surface. Curves (1) and (2): Areas per molecule calculated from $\Delta\sigma_M$ shown in Figure 7 data and charge numbers l given in Figure 8. Curves (3) and (4): Areas per molecule calculated from the reductive desorption model and eq 4. Curves (1) and (3) correspond to the charge density data acquired using the potential step program described in Figure 5b. Curves (2) and (4) correspond to the charge densities determined using the potential step program described in Figure 5c.

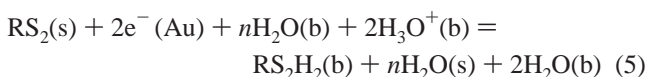
monolayer is adsorbed at the gold electrode and $\sigma_M(-1.2V)$ is the charge density at the potential at which the monolayer is desorbed.

The surface concentrations calculated from the charge density curves for the self-assembled monolayers with the help of eq 4 are also plotted in Figure 9a and the corresponding areas per molecule are plotted in Figure 9b. It is interesting to note that the area per molecules calculated with the help of eq 4 amounts to 55 ± 5 Å² in good agreement with the area per DPTL molecule determined by the “reductive desorption” method in ref 25. As we have already mentioned earlier, this number is lower than the area per molecule calculated from the van der Waals model which is equal to 65 Å² and is physically unreasonable. In conclusion, the “reductive desorption” method gives too high surface densities and too low areas per molecule. The results

(38) Kryszinski, P.; Chamberlain, R. V., II; Majda, M. *Langmuir* **1994**, *10*, 4286–4294.

determined by the reductive desorption method are affected by a significant systematic error.

Why Does the Charge Number per Molecule Depend on the Electrode Potential? In this section, we will explain why the charge number depends on the electrode potential and why it may have values smaller than the number of electrons participating in the “reductive desorption” step. A qualitative discussion of this point was given by Schneider and Buttry.^{28a} We will provide here a rigorous, quantitative explanation. At the metal–solution interface, the reductive desorption is a solvent substitution reaction, and when one thiol molecule is desorbed from the surface n water molecules move from the bulk to the metal surface. In addition, protonation of the desorbed molecule takes place if the pH of the solution is not very high. Instead of the scheme that is usually reported in the literature (shown in eq 1), the “reductive desorption” should be described by



and at equilibrium

$$\mu(\text{RS}_2(\text{s})) + 2\bar{\mu}(\text{e}^- (\text{Au}_{\text{ad}})) + n\mu(\text{H}_2\text{O}(\text{b})) + 2\bar{\mu}(\text{H}_3\text{O}^+(\text{b})) = \mu(\text{RS}_2\text{H}_2(\text{b})) + n\mu(\text{H}_2\text{O}(\text{s})) + 2\mu(\text{H}_2\text{O}(\text{b})) \quad (6)$$

Knowing that the expression for the electrochemical potential is $\bar{\mu}_i = \mu_i + zF\phi$, where μ is the chemical potential and ϕ is the inner potential, eq 6 can be rearranged to take the following form:

$$\mu(\text{RS}_2(\text{s})) - (n)\mu(\text{H}_2\text{O}(\text{s})) + 2\mu(\text{H}_3\text{O}^+(\text{s})) = -2\mu(\text{e}^- (\text{Au}_{\text{ad}})) - (n-2)\mu(\text{H}_2\text{O}(\text{b})) + \mu(\text{RS}_2\text{H}_2(\text{b})) + 2F[\phi(\text{Au}) - \phi(\text{b})] \quad (7)$$

DPTL is an insoluble thiolipid and its desorbed product aggregates into flakes or micelles. The chemical potential $\mu(\text{RS}_2\text{H}_2(\text{b}))$ may be considered as the chemical potential at the critical micelle concentration and the first three terms of eq 7 may be considered to be constant. One may also show that $[\phi(\text{Au}) - \phi(\text{b})] = [E - E_{\text{pzc}}^0] + \text{const}$, where E and E_{pzc}^0 are the actual potential of the gold electrode and the potential of zero charge of the thiol free electrode measured versus a given reference electrode. In the solution of a constant pH, eq 7 may therefore be written in a shorter form

$$\mu(\text{RS}_2(\text{s})) - n\mu(\text{H}_2\text{O}(\text{s})) = 2F[E - E_{\text{pzc}}^0] + \text{const} \quad (8)$$

The chemical potential of a species at the interface is given by³⁹

$$\mu_i(\text{s}) = \mu_i^0(\text{s}) + RT \ln a_i(\text{s}) - A_i\gamma \quad (9)$$

where $A_i = 1/\Gamma_i$ is the area per adsorbed molecule. Using this definition of the chemical potential one can obtain

$$\mu^0(\text{RS}_2(\text{s})) - n\mu^0(\text{H}_2\text{O}(\text{s})) + RT \ln a(\text{RS}_2(\text{s})) - nRT \ln a(\text{H}_2\text{O}(\text{s})) + \frac{\Pi}{\Gamma_{\text{RS}_2}} = 2F[E - E_{\text{pzc}}^0] + \text{const} \quad (10)$$

At a constant DPTL coverage, the terms $RT \ln a(\text{RS}_2(\text{s}))$ and $nRT \ln a(\text{H}_2\text{O}(\text{s}))$ are constant, and eq 8 may be rearranged to give

$$\frac{\Pi}{\Gamma_{\text{RS}_2}} = 2F[E - E_{\text{pzc}}^0] + n\mu^0(\text{H}_2\text{O}(\text{s})) - \mu^0(\text{RS}_2(\text{s})) + \text{const}' \quad (11)$$

A long time ago, Frumkin demonstrated that adsorption of organic molecules causes a change of the interfacial capacity and that this involves work done against the energy stored by the capacitor.^{40,41} The energy stored by the capacitor in the absence of a SAM is equal to

$$w_0 = \frac{1}{2}C_0(E - E_{\text{pzc}}^0)^2 \quad (12)$$

and in the presence of a SAM it is equal to⁴⁰

$$w_1 = \frac{1}{2}C_1(E - E_{\text{pzc}}^1)^2 = \frac{1}{2}C_1(E - E_{\text{pzc}}^0)^2 - C_1E_N(E - E_{\text{pzc}}^0) + \frac{1}{2}C_1(E_N)^2 \quad (13)$$

where C_0 and C_1 are the differential capacities of the interface and E_{pzc}^1 is the potential of zero charge (pzc) of the SAM covered electrode, $E_N = E_{\text{pzc}}^1 - E_{\text{pzc}}^0$ is the shift of the pzc due to the formation of the SAM. The change of the energy of the capacitor contributes to the magnitude of the $\{n\mu^0(\text{H}_2\text{O}(\text{s})) - \mu^0(\text{RS}_2(\text{s}))\}$ term and this contribution is equal to

$$\frac{w_0 - w_1}{\Gamma} = -\frac{C_1E_N(E - E_{\text{pzc}}^0)}{\Gamma} + \frac{1}{2\Gamma}(E_N)^2 - \frac{(C_0 - C_1)}{2\Gamma}(E - E_{\text{pzc}}^0)^2 \quad (14)$$

The potential dependent portion of Π/Γ_{RS_2} is therefore given by

$$\frac{\Pi}{\Gamma_{\text{RS}_2}} = -\frac{C_1E_N(E - E_{\text{pzc}}^0)}{\Gamma} + 2F(E - E_{\text{pzc}}^0) - \frac{(C_0 - C_1)}{2\Gamma}(E - E_{\text{pzc}}^0)^2 + \text{const}'' \quad (15)$$

and recalling eq 3, the charge number l is equal to

$$l = -\frac{1}{F} \left(\frac{\partial \Pi}{\Gamma_{\text{RS}_2} \partial (E - E_{\text{pzc}}^0)} \right)_{\Gamma} = \frac{(C_0 - C_1)}{F\Gamma_{\text{RS}_2}}(E - E_{\text{pzc}}^0) - \frac{C_1E_N}{F\Gamma_{\text{RS}_2}} - 2 \quad (16)$$

The first two terms of eq 16 may be calculated using the experimental charge density and surface concentration data in Figures 5 and 9. For the SAM covered electrode, $\Gamma = 2 \pm 0.2 \times 10^{-10} \text{ mol cm}^{-2}$ within the potential range -0.7 to 0.4V ; $C_1 = 1 \mu\text{F cm}^{-2}$ and the product $C_1E_N = 20 \mu\text{C cm}^{-2}$ since the latter is equal to σ_M for the SAM covered electrode at E_{pzc}^0 . (We note that E_N can be determined by the linear extrapolation of the charge potential curve for the SAM covered electrode to zero charge. In reality, since the product C_1E_N can be read directly from the charge density plot one does not need to determine E_N .) Finally, for each potential E , the values of C_0 can be calculated by differentiation of the charge density curve for the pure supporting electrolyte in Figure 5.

(40) Frumkin, A. Z. *Phys.* **1926**, *35*, 792.

(39) Defay, R.; Prigogine, I.; Bellemans, A.; Everett, D. H. *Surface Tension and Adsorption*; Longmans, Green & Co: London, 1966; p 210.

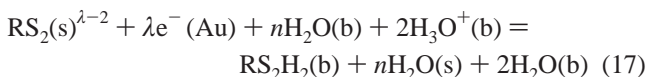
(41) Damaskin, B. B.; Petrii, O. A.; Batrakov, V. V. *Adsorption of Organic Compounds on Electrodes*; Plenum Press: New York, 1971.

The charge number l calculated with the help of eq 16 is plotted in Figure 8 alongside the experimental values of l determined for the film deposited at the electrode surface using the LB method and eq 3. The charge numbers calculated from eq 16 for the SAM covered electrode agree with the experimental values of l determined for the LB film within 10%. The implications of this agreement are significant. It shows unambiguously that, despite the fact that two electrons are flowing to the thiol molecule to reductively desorb it, the actual measured charge per adsorbed molecule may be less than two.

The reason for such unexpected behavior is the presence of a second driving force contributing to the desorption of the thiol molecule. This additional driving force is the work done against the energy stored by the capacitor. Less energy can be stored at the interface when the electrode is covered by SAM than when it is covered by water. This energy loss favors displacement of SAM molecules by water. Consequently, the energy needed to desorb the thiol is less than that provided by the redox reaction (equal to $2FE$) and the effective charge number is less than the number of electrons participated in the redox reaction which in the present case is equal to 2.

An alternative explanation is given by eq 16. It shows that the charge number l has two contributions: one from the electron-transfer step and the second from the recharging of the capacitor caused by desorption of DPTL molecules. The two contributions have opposite signs, and therefore, they cancel each other. The total cancellation takes place at the potential of maximum adsorption where DPTL molecules adsorb without causing a charge to flow to the electrode.

Sometimes a partial charge transfer is invoked to describe the adsorption of a thiol molecule at a gold electrode surface.^{38,42} Therefore, we assume that adsorption of the dithiol molecule at the open circuit potential (during the self-assembly or LB transfer) involves a transfer of $2 - \lambda$ electrons from gold to thiol (gold surface will be positively charged in that case). The cathodic desorption of the adsorbed thiol involves therefore a transfer of λ electrons only. Such reaction is described by



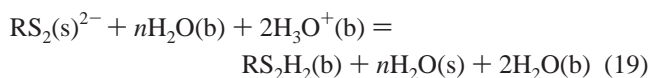
where λ is the partial number of electrons involved in the surface redox reaction during the desorption step. The problem of adsorption with a partial charge transfer has been extensively discussed in the literature.^{43–45} Therefore, we do not need to provide detailed derivation to show that in this case the charge number l is described by the formula

$$l = -\frac{1}{F} \left(\frac{\partial \Pi}{\Gamma_{\text{RS}_2} \partial (E - E_{\text{pzc}}^0)} \right)_{\Gamma} = \frac{(C_0 - C_1)}{F\Gamma_{\text{RS}_2}} (E - E_{\text{pzc}}^0) - \frac{C_1 E_{\text{N}}}{F\Gamma_{\text{RS}_2}} - g_2 - \lambda(1 - g) \quad (18)$$

where $g = (x_2 - x_1)/x_2$ is the geometric factor, with x_1 the distance of the charge center of the adsorbed thiol from the metal surface and x_2 is the thickness of the inner region of the double layer. In the present case, the charge center on adsorbed thiol is located

on the sulfur atom in immediate proximity to the gold surface and x_2 is approximately the thickness of the monolayer which is ~ 4.7 nm thick. Obviously, $x_2 \gg x_1$ and $g \approx 1$, the last term in eq 18 is negligible and the second to last term is equal to -2 . Equation 18 becomes effectively equal to eq 16. Clearly, in the case of adsorption of a long chain thiol molecule, one cannot distinguish between total or partial charge transfer character of the cathodic desorption. The partial charge transfer, if present, would contribute negligibly to the measured electroadsorption valency.

A particular case of desorption with a partial charge transfer corresponding to $\lambda = 0$ occurs when desorption takes place without electron transfer. In this case adsorption at the open circuit potential involves a transfer of two electrons from gold to the dithiol and formation of an adsorbed anion. The cathodic desorption of this anion is then described by a simplified version of eq 17

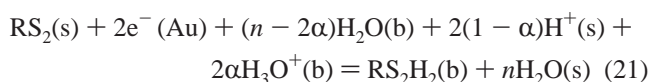


Consequently, the last term in eq 18 disappears and the expression for the charge number l is now given by

$$l = -\frac{1}{F} \left(\frac{\partial \Pi}{\Gamma_{\text{RS}_2} \partial (E - E_{\text{pzc}}^0)} \right)_{\Gamma} = \frac{(C_0 - C_1)}{F\Gamma_{\text{RS}_2}} (E - E_{\text{pzc}}^0) - \frac{C_1 E_{\text{N}}}{F\Gamma_{\text{RS}_2}} - 2g \quad (20)$$

However, since $x_2 \gg x_1$ and $g \approx 1$, eq 20 is effectively equal to eq 16. This is a very significant result. It shows that for a thiol adsorbed at a gold electrode surface, the same value of the charge number (electrodesorption valency) is observed regardless of whether the adsorption involves a surface redox reaction with the total or a partial charge transfer or it is just a simple adsorption of an anion without any electron-transfer step. Clearly, the magnitude of the charge number l (electrodesorption valency) tells us nothing about the oxidation state of the adsorbed species. Consequently, the popular concept of reductive desorption of thiols, described by reaction 1, does not have a strong physical basis. It is prudent not to refer to the desorption of thiols as to a reduction reaction because the redox nature of this process cannot be proven.

In the above discussion, we considered that the adsorbed dithiol is a completely deprotonated molecule and that the protonation reaction takes place in the desorbed state when the molecule resides outside the double layer. Buoninsegni et al.⁴² and more recently Guidelli and Schmickler⁴⁶ considered a model in which the adsorbed monolayer of thiols is partially protonated. In that case, the desorption of a monolayer without partial charge transfer is described by the following equation:



where α is the fraction of and $2(1 - \alpha)\text{H}^+(\text{s})$ is the amount of protons in the adsorbed film of thiols (adsorbed proton). Since $g \approx 1$, in that case, the charge number is given by

(42) Buoninsegni, F. T.; Becucci, L.; Moncelli, M. R.; Guidelli, R. *J. Electroanal. Chem.* **2001**, *500*, 395.

(43) Vetter, K. J.; Schultze, J. W. *Ber. Bunsen-Ges. Phys. Chem.* **1972**, *76*, 920.

(44) Parsons, R. *Can. J. Chem.* **1981**, *59*, 1898.

(45) de Levie, R. *J. Electroanal. Chem.* **2004**, *562*, 273.

(46) Guidelli, R.; Schmickler, W. *Modern Aspects of Electrochemistry*; Conway, B. E., Ed.; Kluwer: New York, 2005; Vol. 38, p 303.

$$l = -\frac{1}{F} \left(\frac{\partial \Pi}{\Gamma_{\text{RS}_2} \partial (E - E_{\text{pzc}}^0)} \right)_{\Gamma} = \frac{(C_0 - C_1)}{F \Gamma_{\text{RS}_2}} (E - E_{\text{pzc}}^0) - \frac{C_1 E_{\text{N}}}{F \Gamma_{\text{RS}_2}} - 2\alpha \quad (22)$$

and for adsorption with a partial charge transfer

$$l = -\frac{1}{F} \left(\frac{\partial \Pi}{\Gamma_{\text{RS}_2} \partial (E - E_{\text{pzc}}^0)} \right)_{\Gamma} = \frac{(C_0 - C_1)}{F \Gamma_{\text{RS}_2}} (E - E_{\text{pzc}}^0) - \frac{C_1 E_{\text{N}}}{F \Gamma_{\text{RS}_2}} - 2g\alpha - \lambda(1 - g) \quad (23)$$

Equation 23 is equivalent to eq 79 in ref 46. In the case of long chain thiols $x_1 \ll x_2$ and $g \approx 1$ and the last two terms on the right-hand side of eq 23 are to a good approximation equal to the last term of eq 22. Consequently, eq 23 derived assuming a partial charge-transfer becomes equal to eq 22, derived assuming adsorption without charge transfer. Therefore, the conclusion that for long chain thiols one cannot distinguish between a partial and a total charge transfer is valid regardless one assumes that the protonation reaction takes place outside the double layer or involves the adsorbed state.

Finally, eq 22 differs from eq 16 because the last term in eq 22 is multiplied by α . The two equations become identical if $\alpha = 1$ (no protonation in the adsorbed state). At this point, we can use experiment to distinguish between the two cases. Figure 8 shows that the measured charge numbers l fit the above equations provided $\alpha = 1$.

4. Summary and Conclusions

We have described a new method to measure the charge number per adsorbed molecule in a monolayer of DPTL self-assembled at a gold electrode surface and the packing density of the SAM. The method relies on chronocoulometric measurement of the charge density at the SAM covered electrode surface. Two series of measurements have to be performed. In the first, the monolayer is deposited onto the gold surface using the LB method. These measurements allow one to determine the charge number per adsorbed DPTL molecule. In the second series, measurements are performed on a self-assembled monolayer. The difference between the charge density of the electrode covered and free of the SAM is measured. The charge numbers determined in the first series are then used to calculate the packing density of the

SAM from $\Delta\sigma$. The area per DPTL molecule determined by this method is about 20% larger than the area calculated from the van der Waals model. This is a reasonable result. In contrast, the popular reductive desorption method gives an area per molecule that is 20% lower than the estimate based on the van der Waals model, which is a physically unreasonable result.

In the reductive desorption method, one assumes that the desorption of a dithiol requires a flow of a constant (potential independent) number of charge units per adsorbed molecule equal to -2 . We have demonstrated that the charge number per adsorbed molecule is not constant but is potential dependent. We have shown that the desorption of DPTL is not only driven by the reductive desorption but also by the work done against the energy stored by the capacitor. Less energy can be stored at the interface when the electrode is covered by a SAM than when it is covered by water. This energy loss favors the displacement of the SAM molecules by water. Consequently, the energy needed to desorb thiol is less than the amount provided by the redox reaction (equal to $2FE$) and the effective charge number is less than the number of electrons participating in the redox reaction. In conclusion, the so-called "reductive desorption" method is based on an incorrect assumption and may lead to significant errors. It should be replaced by the method described in this paper.

We have combined thermodynamic method with Frumkin model of the desorption of DPTL considering three mechanisms: (i) it has a reductive character and involves a transfer of two electrons, (ii) it involves a partial charge transfer, and (iii) it is a simple desorption of anion without electron transfer. The analysis showed that the charge number per adsorbed DPTL, l (electrosorption valency) is described by the same expression regardless of the nature of the mechanism. We have shown that the magnitude of the electrosorption valency cannot provide information about the oxidation state of the adsorbed species. Consequently, the popular concept of "reductive desorption" of thiols does not have a strong physical basis and should not be referred to as to a reduction (a redox) reaction.

Acknowledgment. This work was supported by grants from the Natural Sciences and Engineering Council of Canada and by the National Centre of Excellence in Advanced Foods and Soft Materials. J.L. acknowledges Canada Foundation for Innovation for the Canada Research Chair Award.

LA0535274